lubricants

MDPI

Article

Low Brine Shrimp Bio-Toxicity Marine Lubricating Hydraulic Fluid with Ultra-Low Friction Coefficient and Enhanced Frictional Heat Suppression

Wei Li [1,2], Huanyi Chen [2], Long Chen [2], Shanqin Ge [2], Qingzhao Cai [2], Genxiang Gong [2], Jinhong Yu [2,*], Kazuhito Nishimura [2,3], Nan Jiang [2,*] and Tao Cai [2,*]

1 School of Materials Science and Chemical Engineering, Ningbo University, Ningbo 315211, China; liwei22@nimte.ac.cn
2 State Key Laboratory of Advanced Marine Materials, Ningbo Institute of Materials Technology and Engineering, Chinese Academy of Sciences, Ningbo 315201, China; chenhuanyi@nimte.ac.cn (H.C.); chenlong@nimte.ac.cn (L.C.); geshanqin@nimte.ac.cn (S.G.); caiqingzhao@nimte.ac.cn (Q.C.); gonggenxiang@nimte.ac.cn (G.G.); nishimurakazuhito@nimte.ac.cn (K.N.)
3 Advanced Nano-processing Engineering Lab, Mechanical Engineering, Kogakuin University, Tokyo 192-0015, Japan
* Correspondence: yujinhong@nimte.ac.cn (J.Y.); jiangnan@nimte.ac.cn (N.J.); caitao@nimte.ac.cn (T.C.)

Abstract: Hydraulic technology has been instrumental in the extensive application of offshore mechanical equipment, particularly in drilling platforms and ships, where high-performance hydraulic fluids are essential for safe and efficient operations. Addressing the urgent need for water-based hydraulic fluids as an alternative to traditional oil-based fluids, this study introduces a novel water-based hydraulic fluid fortified with phytic acid, derived from plant seeds, to achieve low biotoxicity, low coefficient of friction, and reduced frictional heat generation. The integration of phytic acid has significantly enhanced the lubricating performance, reducing the average coefficient of friction to as low as 0.013, as tested by the four-ball tester, which is the lowest value reported to date. Real-time monitoring of the temperature rise of the friction testing apparatus using an infrared thermal imager revealed a 78.6% reduction in temperature increase. Acute toxicity assays using Brine Shrimp demonstrated that the 96 h LC50 value for the water–glycol flame-resistant hydraulic fluid with added phytic acid exceeded 26,304 mg/L, indicating low toxicity. Characterization analyses elucidated the mechanisms underlying the improved tribological properties, highlighting the potential of this eco-friendly fluid for safe and efficient offshore operations.

Keywords: Low Brine Shrimp bio-toxicity; ultra-low friction coefficient; frictional heat suppression; marine lubricating hydraulic fluid

check for updates

Received: 21 January 2025
Revised: 20 February 2025
Accepted: 22 February 2025
Published: 26 February 2025

Citation: Li, W.; Chen, H.; Chen, L.; Ge, S.; Cai, Q.; Gong, G.; Yu, J.; Nishimura, K.; Jiang, N.; Cai, T. Low Brine Shrimp Bio-Toxicity Marine Lubricating Hydraulic Fluid with Ultra-Low Friction Coefficient and Enhanced Frictional Heat Suppression. *Lubricants* **2025**, *13*, 103. https://doi.org/10.3390/lubricants13030103

Copyright: © 2025 by the authors. Licensee MDPI, Basel, Switzerland. This article is an open access article distributed under the terms and conditions of the Creative Commons Attribution (CC BY) license (https://creativecommons.org/licenses/by/4.0/).

1. Introduction

"The 21st century is the century of the ocean", the ocean is the main source of resources and spatial guarantee for the long-term development of humanity, society, and nations [1–4]. The development of marine resources heavily relies on offshore engineering equipment. In recent years, with the development and continuous improvement of hydraulic system design and manufacturing technology, the application of hydraulic technology in offshore mechanical equipment has become increasingly widespread [5]. Hydraulic technology plays a significant role in offshore drilling platforms, shipping, and naval vessels. High-performance hydraulic fluids, as an essential part of hydraulic technology, provide strong

support for the safe and efficient operation of hydraulic systems in offshore mechanical equipment [6,7]. However, marine applications demand hydraulic fluids with low biotoxicity, which limits the use of traditional oil-based hydraulic fluids. Consequently, the development of high-performance water-based hydraulic fluids has become one of the current developmental trends.

Water–glycol flame-resistant hydraulic fluid (HFC), known for its excellent biodegradability and low pollution, is widely used in the marine field [8,9]. It has the advantages of being low-price, flame-resistant, and stable. However, it has relatively poor lubricity, which can generate high frictional heat. Friction in mechanical equipment is an inevitable phenomenon that causes significant energy loss [10,11]. The energy consumed by friction is converted into the form of frictional heat and dissipated. Under high shear and high-pressure conditions, a high coefficient of friction (COF) of the lubricant can lead to energy being dissipated in the form of heat, a rapid increase in the operating temperature of the lubricant, and lubrication failure [12,13]. Therefore, it is crucial to reduce friction in mechanical equipment and minimize energy loss as part of the response to the current energy crisis [14–16].

In industry, friction modifiers are often added to improve the tribological performance of lubricating oils [17–20]. Traditional petroleum-based friction modifiers not only struggle with solubility in water-based systems but also pose significant environmental challenges due to their inherent non-degradability and the use of toxic additives such as chlorides, sulfides, and fluorides, which contribute to environmental and aquatic pollution [21–23]. Therefore, screening for green and environmentally friendly friction-improving additives and optimizing the formulation can not only enhance the lubricating performance of water–glycol flame-resistant hydraulic fluids and reduce the generation of frictional heat during motion but also facilitate the better application of water–glycol flame-resistant hydraulic fluids in marine hydraulic environments.

In this study, a novel phytic acid-based full-formulation water-based hydraulic fluid was developed by optimizing the formulation of phytic acid, thickeners, and additive package to prepare a water–ethylene glycol hydraulic fluid [24]. The testing principle of the four-ball machine mainly involves placing four steel balls in a specific arrangement (typically three balls as the lower balls and one as the upper ball) within the testing device, applying a certain load, and rotating one of the balls. By simulating the frictional contact under actual working conditions, it measures parameters such as friction force and friction coefficient to evaluate the tribological properties of lubricants. The friction performance was tested using a four-ball friction test, and it was found that the coefficient of friction was as low as 0.013, which is the lowest value reported to date for water-based hydraulic fluids tested using similar methods. Additionally, thermal imaging technology was used to monitor the generation of frictional heat during the friction process, and the low coefficient of friction significantly reduced the generation of frictional heat, with a notable 78.6% decrease in the temperature rise of the test oil. The biocompatibility of the fluid was confirmed through Brine Shrimp lethality tests, demonstrating the excellent biological compatibility of the oil sample [25,26]. The Brine Shrimp lethality test is a rapid toxicity detection method based on the nauplii of Artemia salina (Brine Shrimp). It assesses the potential biological activity or toxicity of a test substance by evaluating its lethal effects on Brine Shrimp. The core indicator is the median lethal concentration (LC50), where a lower value indicates stronger toxicity. Moreover, we employed a variety of characterization methods to explain how the addition of phytic acid (PA) to our self-prepared water–glycol flame-resistant hydraulic fluid significantly enhanced its lubricating performance, A possible lubrication mechanism was discovered and investigated in detail [27,28]. It was found that during the friction process, the lubrication film generated converts into

fine particles, which participate in frictional chemical reactions to promote lubrication effectiveness [29,30].

2. Materials and Methods

2.1. Materials

The phytic acid solution with a concentration of 70% was purchased from Aladdin Group Chemical Reagent Co., Ltd., Shanghai, China. The purchased phytic acid solutions were mixed with commercially available components (deionized water, ethylene glycol, diethylene glycol, polyether, and an additive package) to obtain water–ethylene glycol fire-resistant hydraulic fluids at weight ratios of 1.0, 2.0, 4.0, and 8.0 wt% to prepare mixtures, respectively labeled as HFC-PA-1 (Table 1), HFC-PA-2, HFC-PA-4, HFC-PA-8. The water-ethylene glycol flame-retardant hydraulic fluid without the addition of phytic acid solution will serve as a blank control and will be labeled as HFC-PA-0.

Table 1. The parameter conditions of HFC-PA-4 and Castrol.

	HFC-PA-4	**Castrol**
ISO Viscosity Grade	46	46
Specific Gravity @15 °C (g/cm^3)	1.08	1.07
Kinematic Viscosity 40 °C (mm^2/s)	47	48
Pour Point (°C)	−45	−51
Flash Point (°C)	None	None

2.2. Friction Experiments

Friction performance tests were conducted using a four-ball friction tester (MS-10 A, Tenkey, Xiamen, China, China). Prior to the friction test, the steel balls were treated with an anhydrous ethanol solution through ultrasonic processing to remove surface contaminants. Additionally, to ensure the accuracy of the four-ball test, a more precise sensor was employed. The test conditions for this experiment were set at 50 N, using a friction sensor (Xiamen Tianji Co., Ltd., Xiamen, China, MS-10A) with a precision of 1 g and a lever amplification device (with a magnification factor of 27.276 times) was connected to the friction transmission mechanism and the sensor. For each friction test, GCr15 steel balls were used. The lubricants used were formulated HFC-PA-0, HFC-PA-1, HFC-PA-2, HFC-PA-4, HFC-PA-8, and two commercially available water–ethylene glycol fire-resistant hydraulic fluids. To ensure the accuracy of the tribological data, each experiment was repeated three times, with a recording accuracy of ±0.001 for the friction coefficient. All tests were conducted in an air environment at room temperature and a relative humidity of 30–50%.

2.3. Characterization Methods

Using the TA Instruments ARG2 rotational shear rheometer, the rheological behavior was tracked under shear rates ranging from 0 to 100 s^{-1}. Thermal imaging videos of the friction pr°Cess were captured using an infrared camera (Fluke Ti392, Washington, DC, USA), and the lubrication film on the cross-section of the worn steel balls was analyzed using f°Cused ion beam (FIB, Auriga, Eschborn, Germany) and high-resolution transmission electron microscopy (HR-TEM, Talos F200X, Waltham, MA, USA). The elemental composition and chemical state of the lubrication film formed on the surface of the worn steel balls were analyzed using X-ray photoelectron spectroscopy (XPS, AXIS SUPRA, Kratos, Tokyo, Japan). The chemical composition of the wear area on the steel ball was analyzed using Time-of-Flight Secondary Ion Mass Spectrometry (TOF-SIMS, SurfaceSeer I, Kore,

Oxfordshire, UK). The distribution of fine particles near the worn steel balls was observed using scanning electron microscopy (SEM, Zeiss G300, Oberkochen, Germany). The height of fine particles and the roughness of the worn area were analyzed using atomic force microscopy (AFM, Bruker, Billerica, MA, USA). A contact angle meter (DSA100, KRUSS, Hamburg, Germany) was used to measure the contact angle between the lubricant and the steel plate.

2.4. Biological Toxicity Testing

We have designed a low-toxicity hydraulic fluid for marine vessels, which is used in mechanical equipment operating in marine environments. It has good lubricating properties, is environmentally friendly, and reduces the generation of frictional heat in the system. In the use of various marine equipment, it is inevitable to encounter the problem of oil leakage. Traditional oil-based hydraulic fluids have poor biotoxicity, and once leaked, they can cause serious harm to marine life. The low-toxicity marine hydraulic fluid used in this research has good biotoxicity and is environmentally friendly. Even in the event of a leak, the impact of the low-toxicity marine hydraulic fluid on marine life. is minimal.

The Brine Shrimp Acute Toxicity Test was employed to assess the biotoxicity, with five different concentrations of the test sample solution (HFC-PA-4, Castro) and a blank solution prepared. The static exposure method was used for the test, which lasted for a total of 96 h without feeding during the experimental period. 100 mL of the test solution and 40 Brine Shrimp were placed in covered glass beakers and incubated in a culture chamber for the experiment. Observations and records of the Brine Shrimp and mortality were made daily from the start of the experiment. Parameters such as pH, salinity, and dissolved oxygen of the test solution were measured and recorded at the beginning and end of the experiment.

Validity of the experiment: At the end of the experiment, the mortality rate of the Brine Shrimp in the blank control group was 0%, the dissolved oxygen in the test solution ranged from 86.2% to 99.9%, the test temperature ranged from 24.9 °C to 25.6 °C, the salinity was between 30 ppt and 31 ppt, and the pH ranged from 7.78 to 8.15. These parameters met the quality control requirements for the test standards (the mortality rate of Brine Shrimp in the blank control group should not exceed 10%, the dissolved oxygen saturation of the test solution should be greater than 60%, the water temperature change during the test period should not exceed 2 °C, the salinity change should not exceed 2, and the pH change range should not exceed 0.4; therefore, the results of this experiment are valid.

3. Results

3.1. Frictional Properties

The four-ball friction tester plays a significant role in the industrial sector, is commonly used for the evaluation and control of industrial product quality, and is the standard equipment for testing the frictional properties of water–glycol flame-retardant hydraulic fluids. In this study, a four-ball friction tester was selected to conduct friction tests at 392 N and 1200 r/min to better approximate actual working conditions for the research. Additionally, to ensure the accuracy of the four-ball test, a more precise sensor was employed. The friction sensor used in this experiment (Xiamen Tianji, Ltd., MS-10A) has an accuracy of 1 g. As shown in Figure 1a, under conditions of 392 N pressure and 1200 r/min rotational speed (corresponding to an initial contact pressure of 2.3 GPa), the frictional properties of water–glycol fire-resistant hydraulic fluid with different concentrations of PA additives were tested. Here, HFC-PA-0, HFC-PA-1, HFC-PA-2, HFC-PA-4, and HFC-PA-8 represent solutions with mass concentrations of phytic acid additives at 0%, 1.0%, 2.0%, 4.0%, and 8.0%, respectively. Significantly, the tribological assessment revealed that with the HFC-PA-4 formulation enriched with 4.0% phytic acid, an ultra-low friction coefficient was achieved.

The average friction coefficient of HFC-PA-4 was recorded at an exceptionally low value, which is 0.013. Upon observing a significant deterioration in lubrication performance following the addition of 8% phytic acid (PA), we propose the following explanations for this phenomenon: Phytic acid's six phosphate groups adsorb onto steel surfaces, forming a protective lubricating film. At 4% PA, optimal adsorption occurs, creating a dense, uniform amorphous film. However, at 8% PA, excessive molecules may saturate surface sites, leading to overcrowding and weaker intermolecular interactions. This results in a fragmented or inhomogeneous film, exposing the steel substrate intermittently and increasing friction. TOF-SIMS and XPS data confirm PA's role in forming $FePO_4$ and P–O bonds, but over-saturation likely disrupts film cohesion, as observed in similar studies [23]. High PA concentrations may intensify tribochemical reactions under high-pressure conditions (392 N, 1200 rpm). Excess PA could decompose into free phosphate ions or form brittle $FePO_4$ phases. These byproducts might act as abrasives, accelerating wear and increasing friction. In Figure 1b, We selected a leading hydraulic fluid in the international market, Castrol (Table 1), to conduct a friction test alongside HFC-PA-4 under the test conditions of 392 N and 1200 r/min for half an hour. The friction coefficient of HFC-PA-4 was significantly lower than that of Castrol, indicating that HFC-PA-4 possesses superior lubricating performance. In Figure 1c, we reviewed previously published work that shares the same test conditions as this work. We compared the friction coefficients of these studies with those of this work and found that the friction coefficient of this work is the lowest, reaching the level of an ultra-low friction coefficient. This indicates that, under the four-ball friction test conditions, the friction coefficient performance of this work has an advantage.

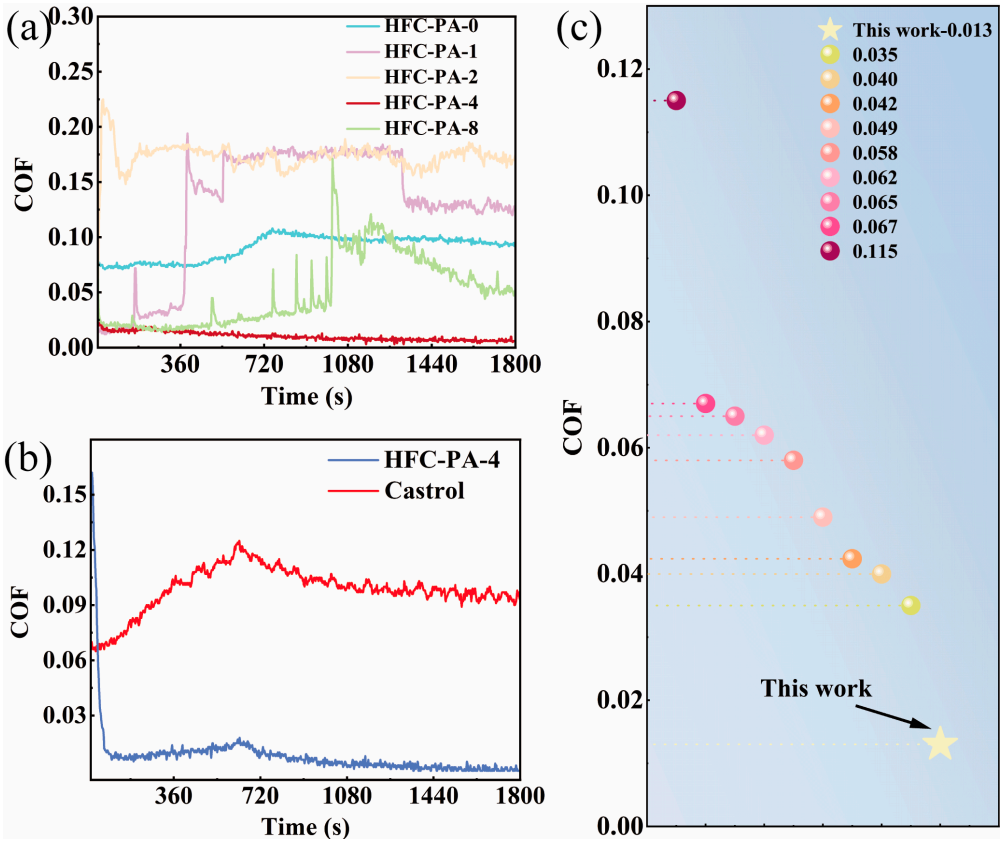


Figure 1. (**a**) Coefficient of friction curves of HFC-PA-0, HFC-PA-1, HFC-PA-2, HFC-PA-4, and HFC-PA-8 under a load of 392 N with a speed of 1200 r/min. (**b**) The friction coefficient curves of HFC-PA-4 and the internationally leading commercial hydraulic fluid Castrol under the conditions of 392 N and 1200 r/min, (**c**) Under the test conditions of 392 N and 1200 r/min, the comparison of friction coefficients of lubricants from different literature sources is as follows [31–39].

3.2. The Relationship Between the Friction Coefficient and Frictional Heat

The energy expended to counteract friction is transformed into thermal energy, which is then dissipated into the lubricant and machinery, consequently leading to an elevation in temperature for both the lubricant and the mechanical components. An increase in the temperature of the water-based lubricant exacerbates its volatility, reducing its long-term lubricating effectiveness. Meanwhile, an increase in the temperature of the mechanical equipment shortens its lifespan and reduces its stability. Therefore, studying frictional heat is of significant practical importance, providing a feasible solution to address energy loss issues.

In this work, we investigated the generation of frictional heat in different hydraulic fluids during friction tests. We believe that the majority of the frictional heat is transferred to the oil and the frictional equipment, so we used the temperature rise of the lubricant and the equipment to reflect the amount of frictional heat generated. This study selected three different hydraulic fluids: HFC-PA-4, HFC-PA-0, and Castrol. To better demonstrate the differences in frictional heat generation among the various hydraulic fluids, we extended the friction test duration to 1 h, conducting the friction tests under room temperature, a load of 392 N, and a rotational speed of 1200 r/min. Thermal imaging was used to observe the temperature of the equipment (oil cup), while the built-in temperature detection device of the four-ball friction tester was used to measure the temperature of the lubricant.

After one hour of friction testing, the temperature rises for HFC-PA-4, HFC-PA-0, and Castrol were 9.0 °C, 32.9 °C, and 35.4 °C, respectively (Figure 2a). From the thermogram in Figure 2b, it can be seen that after one hour of friction testing, the temperature increases the equipment for HFC-PA-4, HFC-PA-0, and Castrol reached 6.1 °C, 28.6 °C, and 34.5 °C, respectively. We can observe that after one hour of friction, the temperature rise of both the oil liquid and the equipment for HFC-PA-4 is significantly lower than that for HFC-PA-0 and Castrol. This indicates that the frictional heat generated by HFC-PA-4 is much less than that of HFC-PA-0 and Castrol. The low frictional heat characteristic of HFC-PA-4 is closely related to its ultra-low coefficient of friction, as frictional heat is produced by the work conducted by frictional forces. In engineering applications, the low frictional heat characteristic of HFC-PA-4 can extend the service life of hydraulic fluids and ensure the normal operation of machinery and equipment.

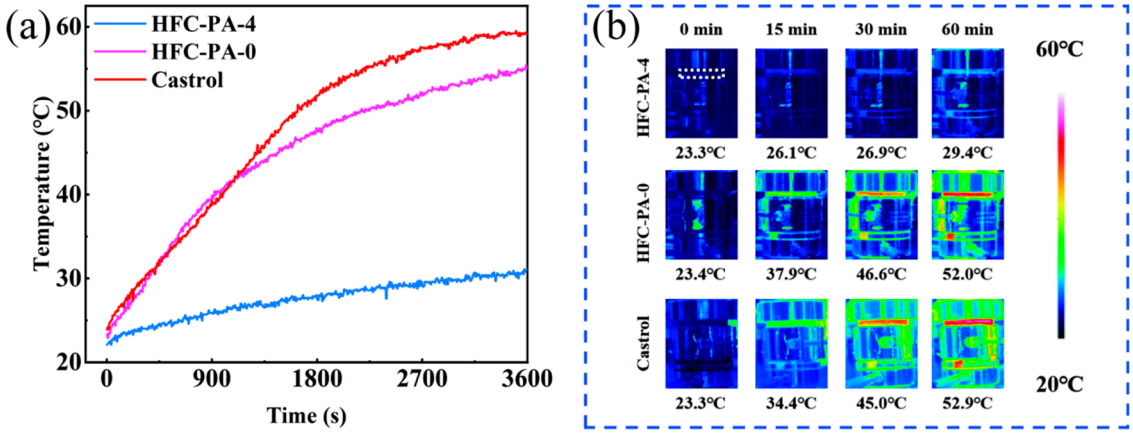


Figure 2. The experiment was conducted under conditions of a 392 N load and a rotational speed of 1200 revolutions per minute, (**a**) Temperature curves of lubricants (HFC-PA-4, HFC-PA-0, and Castrol), (**b**) Thermal images of equipment with HFC-PA-4, HFC-PA-0, and Castrol lubricants.

3.3. Biotoxicity Testing for HFC-PA-4

Experimental results: Acute toxicity tests conducted with Brine Shrimp indicated that through linear regression analysis of the experimental data, the 96 h LC50 (median lethal

concentration) for HFC-PA-4 is approximately 26,304 mg/L, and for the commercial product Castrol, it is approximately 23,795 mg/L. Both meet the GB/T 18420.2-2001 standard and can be discharged directly into the ocean, demonstrating good biological toxicity and environmental friendliness (Figure 3b).

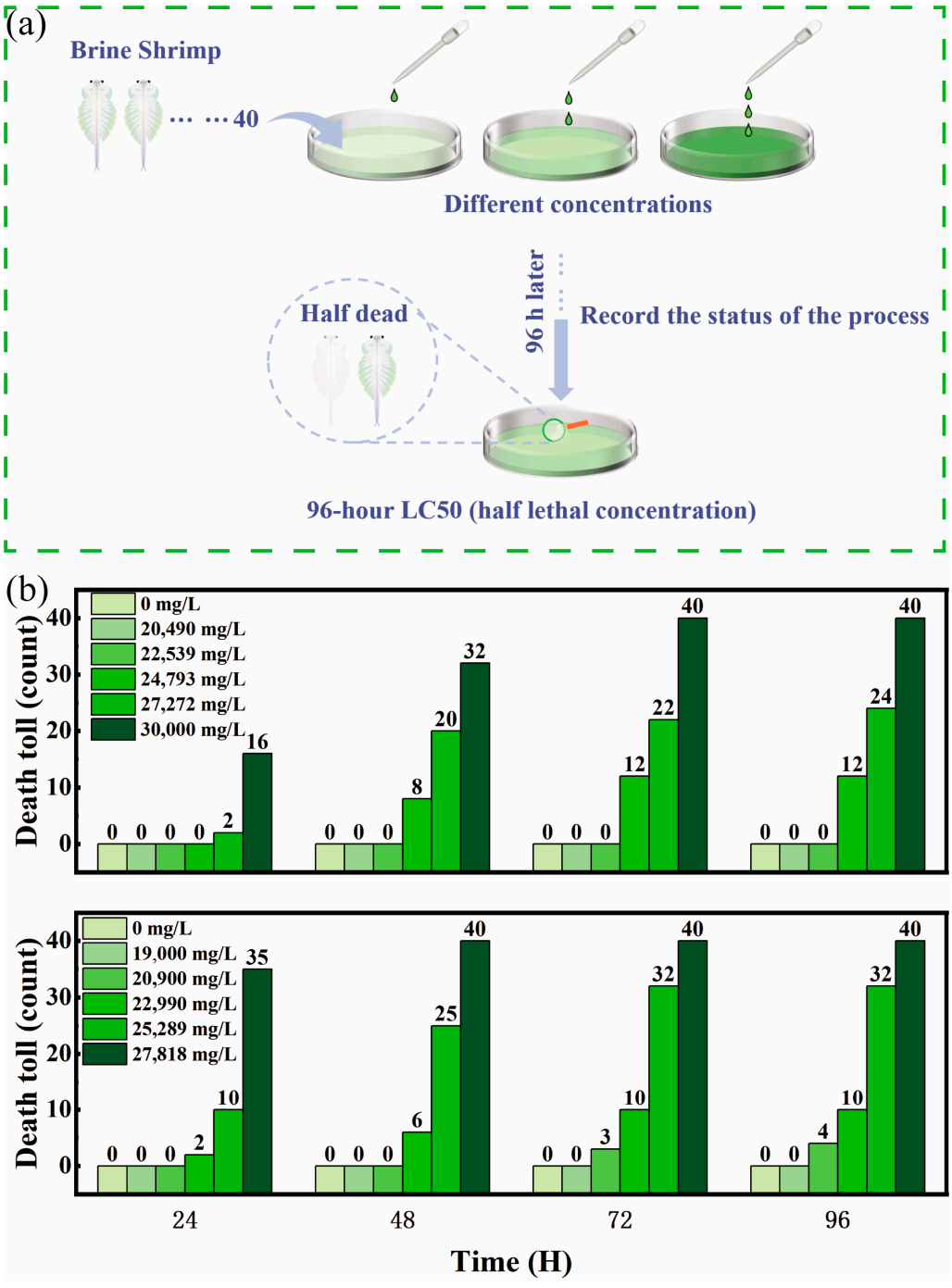


Figure 3. (**a**) Biological toxicity testing method schematic diagram and (**b**) biological toxicity test results for HFC-PA-4 and Castrol.

The results show that: The 96 h LC50 (median lethal concentration) of HFC-PA-4 is greater than that of Castrol, which indicates that HFC-PA-4 has lower biological toxicity compared to Castrol and is more environmentally friendly and harmless. The bio-toxicity results of HFC-PA-4 indicate that it can be directly discharged into the open sea, effectively mitigating the marine pollution caused by oil spills.

3.4. Friction Mechanism Analyses

The detailed condition of the lubricating film formed after a 30 min friction test of GCr15 steel balls under the test conditions of 392 N and 1200 r/min were analyzed using HRTEM. As shown in Figure 4a, a section of the wear track on the GCr15 steel balls lubricated with HFC-PA-0 was extracted using FIB, revealing layers 1# and 2# as two different Pt layers on top, with layer 3# being the lubricating film and layer 4# representing the steel substrate. Figure 4b indicates that layer 3# does not exhibit lattice fringes. Figure 4c,d shows the corresponding element content displayed by EDS, indicating a lower Fe content in the lubricating film layer compared to the steel substrate, while the carbon and oxygen content is higher. These results indicate that after 30 min of friction testing, a lubricating film with a thickness of approximately 7 nm is formed on the surface of the GCr15 steel balls lubricated with HFC-PA-0.

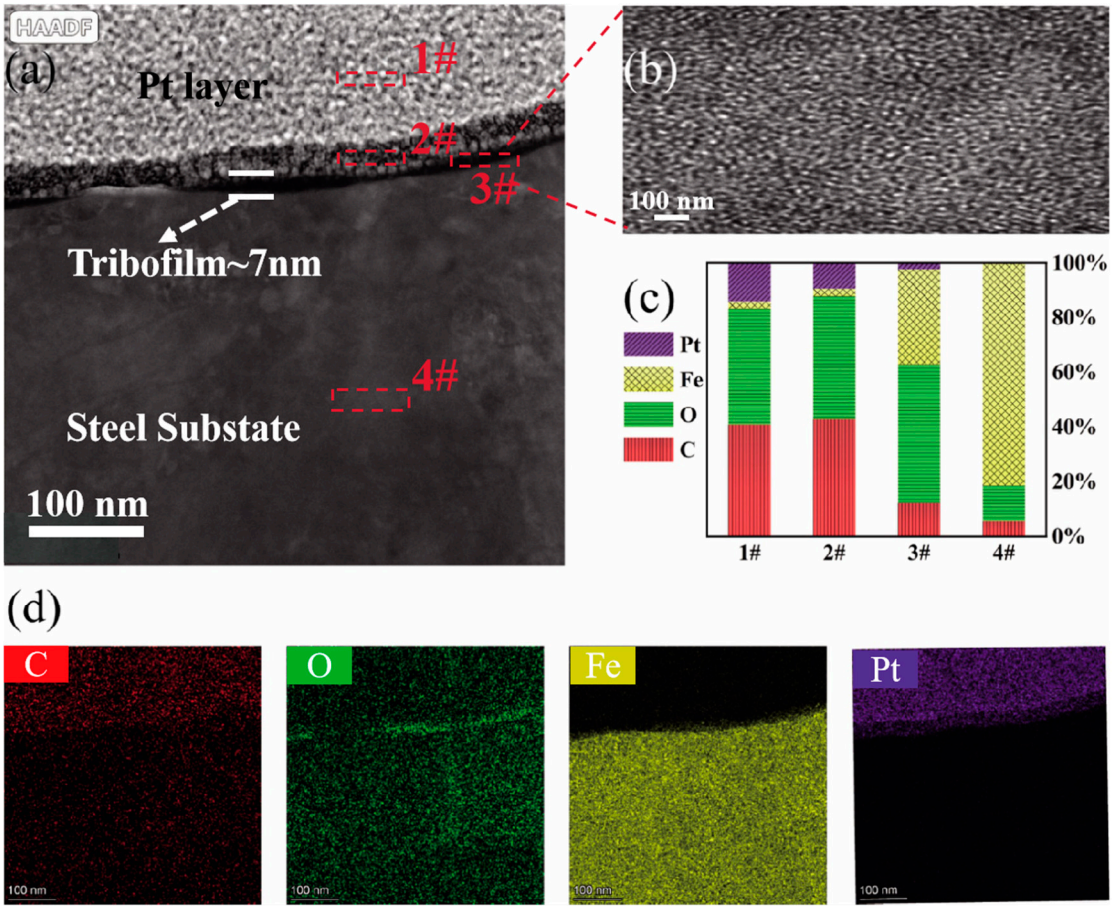


Figure 4. (**a**) Cross-sectional TEM image of worn surface lubricated by HFC-PA-0, (**b**) Crystal lattice image at position 3#, (**c**) Elemental content at different positions corresponding to TEM images, and (**d**) Corresponding EDX elemental map of TEM images.

Similarly, as shown in Figure 5a, a section of the wear track on the GCr15 steel balls lubricated with HFC-PA-4 was extracted using FIB. The section revealed layers 1# and 2# as two different Pt layers on top, with layer 3# being the lubricating film and layer 4# representing the steel substrate. Figure 5b,c indicate that layer 3# exhibits no lattice fringes, indicating an amorphous structure. Figure 5d,e shows the corresponding element content displayed by EDS, indicating a lower Fe content in the lubricating film layer compared to the steel substrate, while the carbon and oxygen content is higher. Unlike the lubricating film produced by HFC-PA-0, the lubricating film produced by HFC-PA-4 contains a significant enrichment of P elements, and the thickness of the lubricating film

increases from 7 nm without PA addition to 392 nm with 4% mass concentration of PA. This is because the addition of a 4% mass concentration of PA enhances the adsorption capacity of HFC-PA-4 to the GCr15 steel substrate.

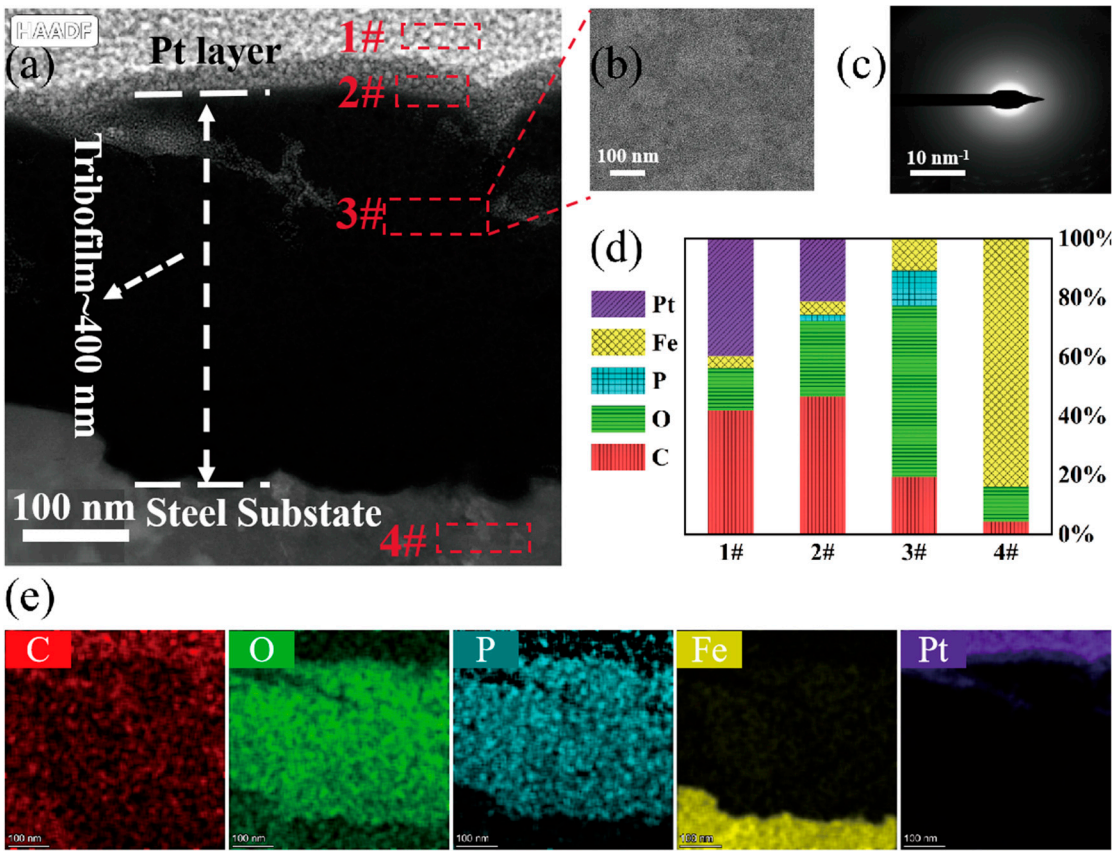


Figure 5. (**a**) Cross-sectional TEM image of worn surface lubricated by HFC-PA-4, (**b**,**c**) Crystal lattice image and diffraction pattern at position 3#, (**d**) Elemental content at different positions corresponding to TEM images, (**e**) Corresponding EDX elemental map of TEM images.

Utilizing a four-ball friction tester, we performed friction tests on HFC-PA-4, supplemented with PA, at room temperature (392 N, 1200 r/min) for a duration of 30 min. Subsequently, X-ray photoelectron spectroscopy (XPS) was meticulously applied to analyze the elemental composition and chemical states within the wear track region on the steel balls. The wide-scan XPS spectrum depicted in Figure 6a reveals the presence of carbon, phosphorus, oxygen, and iron elements. The C 1 s spectrum in Figure 6b presents peaks at binding energies of 284.80 eV, 286.29 eV, and 288.45 eV, which are indicative of the C-C, C-O-C and O-C=O bonds, respectively. The P 2p spectrum depicted in Figure 6c exhibits peaks at binding energies of 133.13 eV and 134.00 eV, which are attributed to the P 2p1/2 and P 2p3/2 energy levels, respectively. The energy separation of 0.87 eV between these peaks is characteristic of phosphorus within the FePO4 compound [40,41]. The O 1 s spectrum in Figure 6d exhibits peaks at 526.66 eV, 531.18 eV, and 532.73 eV, which are associated with Fe_2O_3, P-O bonds, and oxygen in adsorbed oxygen species [40], respectively. Lastly, the Fe 2p spectrum in Figure 6e illustrates peaks at 710.26 eV, 723.36 eV, 712.50 eV, and 725.60 eV. The peaks at 710.26 eV and 723.36 eV are assigned to Fe 2p3/2 and Fe 2p1/2 in Fe_2O_3, respectively, showcasing an energy gap of 13.1 eV. Similarly, the peaks at 712.50 eV and 725.60 eV are ascribed to Fe 2p3/2 and Fe 2p1/2 in FePO4 [41,42], respectively, maintaining the same energy difference of 13.1 eV. These XPS findings suggest that after a half-hour of friction testing at room temperature (392 N, 1200 r/min), a reaction occurred on the surface

of the GCr15 steel balls involving the phosphoric acid groups from the added phytic acid, which in turn bolstered the adherence of the solution to the steel balls.

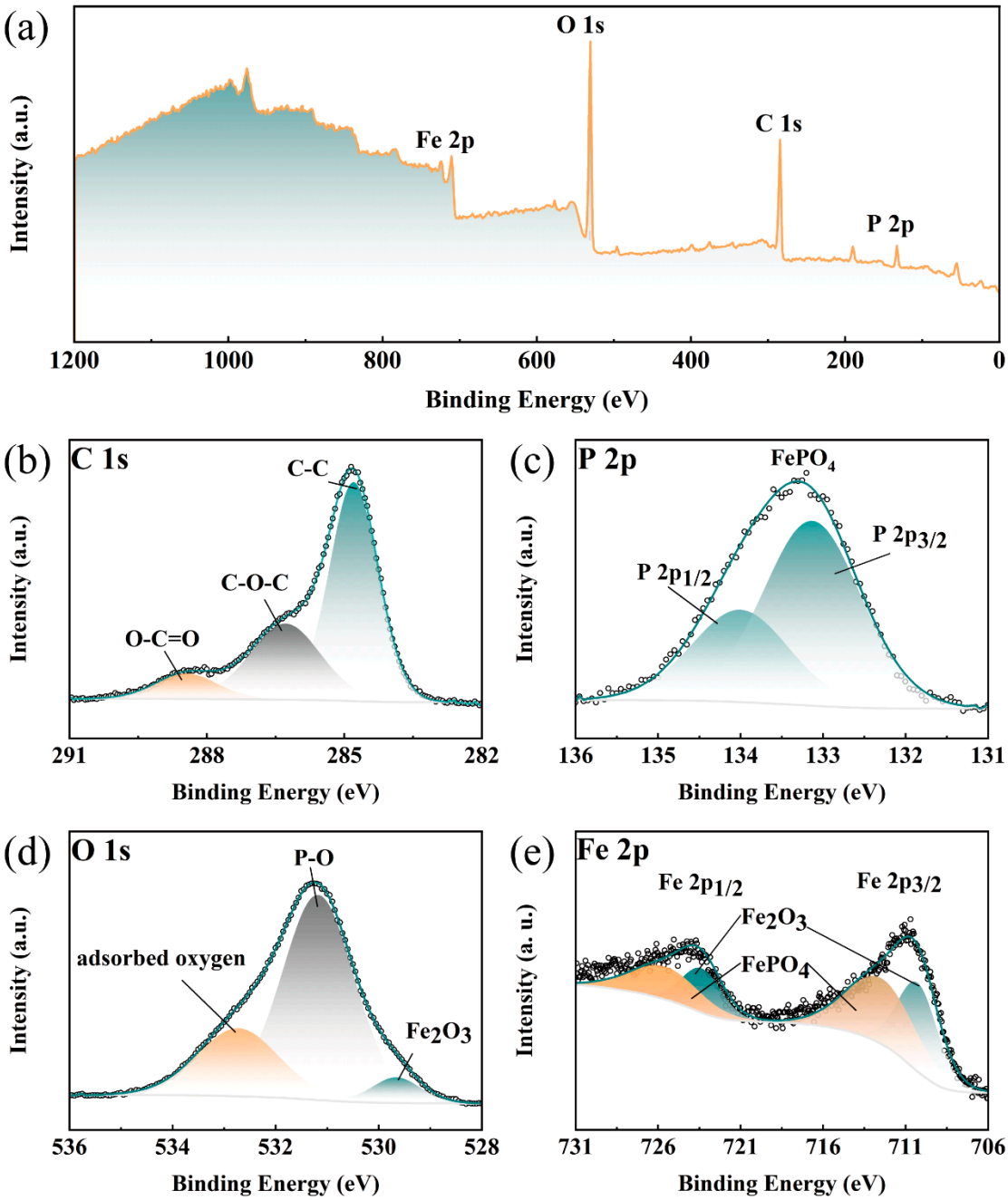


Figure 6. XPS spectra of the steel balls wear track surface when using HFC-PA-4 solution as a lubricant: (**a**) Overview, (**b**) C 1s, (**c**) P 1p, (**d**) O 1s, and (**e**) Fe 2p. The applied load during the friction test was 392 N, the rotational speed was 1200 r/min, and the test duration was 1800 s.

The Time-of-Flight Secondary Ion Mass Spectrometry (TOF-SIMS) is one of the most powerful tools for characterizing the chemical composition of friction films formed during frictional reactions [43,44]. Figure 7. depicts the characterization of the friction film formed on the location of the worn spot on steel balls after conducting a 30 min friction test (392 N, 1200 r/min) with HFC-PA-4 containing 4 wt% PA, using TOF-SIMS. Figure 7a illustrates the anion and cation spectra of the friction film, with the x-axis representing the mass-to-charge ratio, where different ratios represent different ion fragments. In the anion spectrum, characteristic peaks of phosphorus-containing ion fragments, such as

P^-, PO^-, PO^{2-}, and PO^{3-}, are detected, indicating the involvement of phytic acid in the frictional chemical reaction on the surface of GCr15 steel balls. In the cation spectrum, Fe+ is detected, suggesting its association with P (P^-, PO^-, PO^{2-}, PO^{3-}) on the friction surface, which is closely related to the formation of the lubricating film. A significant amount of carbon–hydrogen ion fragments ($CxHy^+$) is observed in the cation spectrum, which may originate from the decomposition of phytic acid and other components in HFC-PA-4. Figure 7b displays the two-dimensional TOF-SIMS image of the lubricating film on the worn spot within the 150 μm × 150 μm range, showing both anions and cations (P^-, PO^-, PO^{2-}, PO^{3-}, OH^-, O^-, Fe^+, $CxHyO^+$, $CxHy^+$). The high intensity of anions (PO^{3-}, PO^2, PO^-, Fe^+) suggests the chemical reaction between the phosphate groups in phytic acid and the steel ball surface, proving the occurrence of frictional chemical reactions involving phytic acid during friction. It is speculated that this might be one of the reasons for the significant increase in the thickness of the TEM friction film, indicating that the addition of phytic acid facilitates the formation of the lubricating film [45,46].

After conducting a 30 min friction test on HFC-PA-0 and HFC-PA-4 under conditions of 392 N and 1200 rpm, we observed using a scanning electron microscope (SEM) that the wear track of HFC-PA-4 was surrounded by densely packed fine particles (see Figure 8b1,b2), while no such particles were present around the wear track of HFC-PA-0 (see Figure 8a1,a2). To verify whether the presence of these particles was coincidental, we performed additional friction tests on HFC-PA-4 under the same conditions for 7.5, 15, 30, and 60 min (see Figure 8c) and then observed the wear tracks using SEM. We found that fine particles of similar size appeared in all different durations of the friction tests, indicating that the presence of these fine particles is not coincidental but is part of the friction chemical reaction.

We used an atomic force microscope (AFM) to analyze the fine particles near the wear track of HFC-PA-4 after a 30 min friction test under the same conditions. Figure 8d1,d2 show the 2D and 3D imaging of the fine particles under AFM, indicating that the particles are densely distributed and have a certain height. Figure 8d3, which is the particle size distribution chart from Figure 8d1, shows that the particle size primarily ranges within 0.617 ± 0.323 μm. Figure 8d4, which selects four particles from Figure 8d1, displays the height of these fine particles, finding that their height is about 280 nm [47].

We also conducted an EDS analysis on fine particles. Since these small particles are distributed on the surface of GCr15 steel balls, directly analyzing the small particles on the steel balls using EDS would be inaccurate due to interference from the steel balls. Therefore, we collected GCr15 steel balls that had undergone friction testing with HFC-PA-4 for 30 min under conditions of 392 N and 1200 rpm and then subjected the steel balls to ultrasonication in ethanol. To ensure the accuracy of the tests, we used SEM and TEM for analysis and cross-validated the results of both methods. The ethanol solution after ultrasonication was dripped onto a silicon wafer and dried, followed by EDS analysis using SEM (Figure 8e), while the ethanol lubricant after ultrasonication was analyzed using TEM for EDS analysis (Figure 8f). The EDS results from SEM and TEM showed basic consistency, and we also found that the elemental content of the small particles was consistent with the lubricant content in Figure 4a. Therefore, we can confirm that the small particles originate from the lubricant film generated by frictional chemical reactions. In summary, we infer that during the friction process, the phosphate groups (PO_4^{3-}) in PA react with the steel ball surface (Fe) to form a non-dense lubricating film, which is confirmed by the results of XPS and TOF-SIMS. Under the action of shear force, the lubricating film is stripped off and forms fine particles (Figure 8). The elemental composition of these fine particles is very close to that of the lubricating film, which confirms that the fine particles originate from the lubricating film. Subsequently, these fine particles flow with the lubricating oil

and participate in the friction process. This is because the fine particles originate from the lubricating film but are also present in large quantities near the wear track.

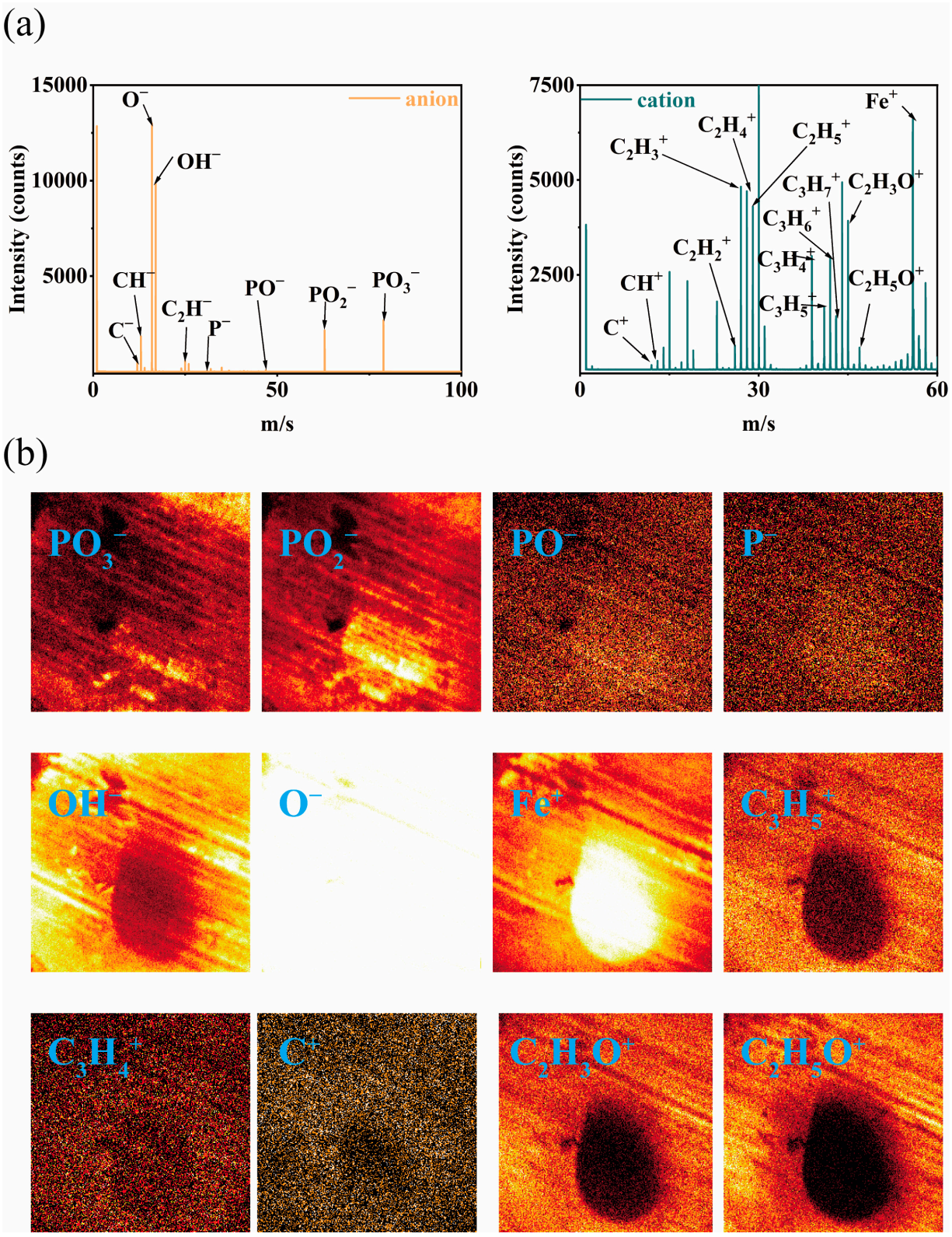


Figure 7. Lubrication film on the worn surface lubricated by HFC-PA-4: (**a**) TOF-SIMS mass spectrum and (**b**) TOF-SIMS imaging of positive and negative ions. (The mass spectrometry area mapping is 150 μm × 150 μm).

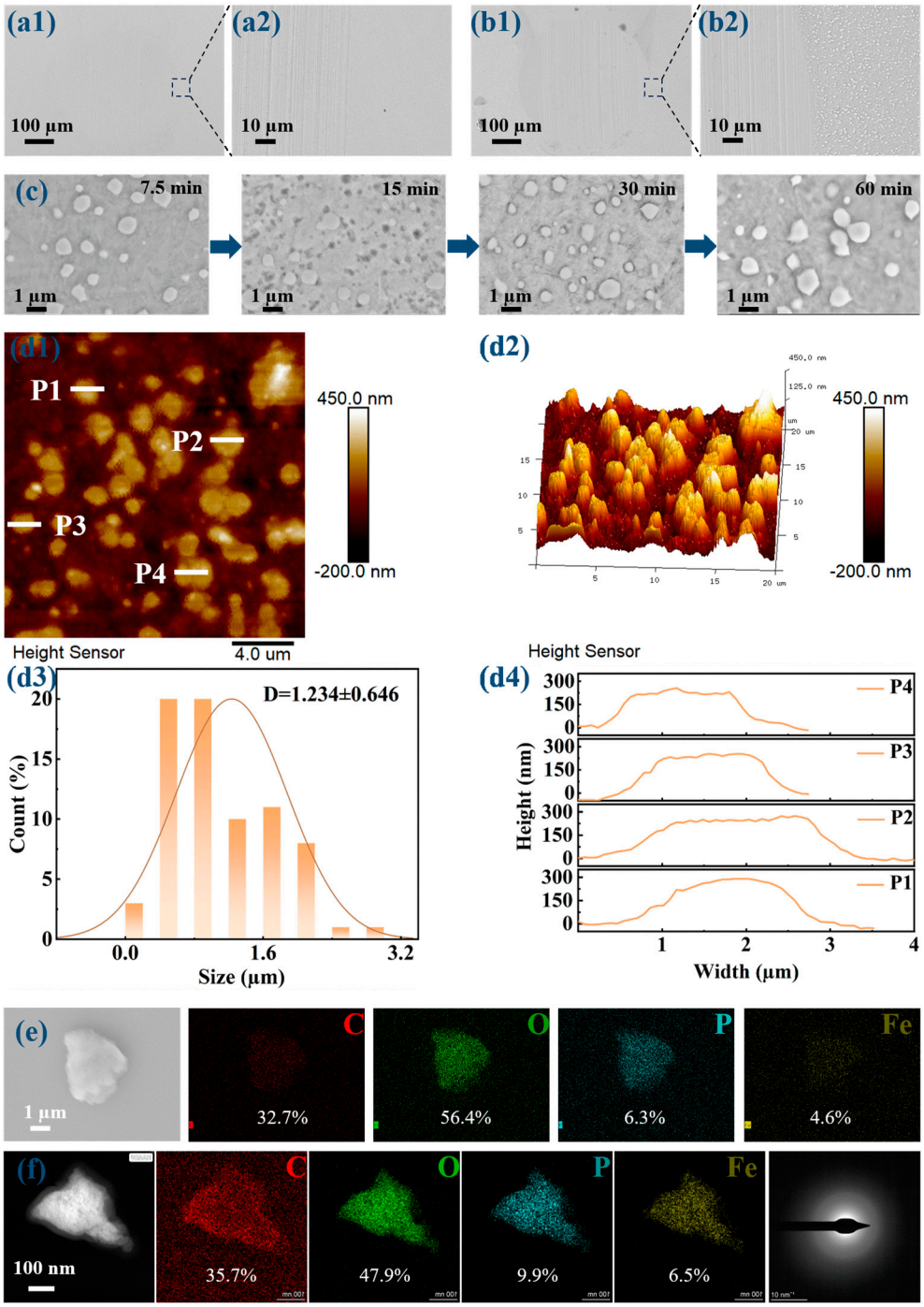


Figure 8. (**a1**,**a2**) SEM images of wear tracks lubricated by HFC-PA-0 and their magnified edges, (**b1**,**b2**) SEM images of wear tracks lubricated by HFC-PA-4 and their magnified edges, (**c**) SEM images of fine particles after HFC-PA-4 lubrication for 7.5, 15, 30, and 60 min, (**d1**,**d2**) 2D and 3D images of fine particles under AFM, (**d3**) Statistical analysis of fine particle sizes, (**d4**) Height profile of four selected fine particles, (**e**) EDS mapping of fine particles on a silicon wafer under SEM, and (**f**) EDS mapping of fine particles under TEM.

As previously mentioned, the hydraulic fluid (HFC-PA-4), with the addition of phytic acid solution, forms a lubricating film with a thickness of up to 400 nm during the friction process (Figure 4), which far exceeds the thickness of the lubricating film formed by the hydraulic fluid without phytic acid (HFC-PA-0). This is due to the strong adsorption effect of the phosphate groups in phytic acid on metal24. We have also verified this point; from Figure 9, it can be observed that the contact angle of the HFC-PA-4 solution with phytic

acid on a steel plate of the same material as the steel ball is 35°, which is significantly smaller than the contact angle of 54° for the HFC-PA-0 solution without phytic acid. A lower contact angle indicates a stronger affinity, which is the reason why the lubricating film formed by (HFC-PA-4) can reach a thickness of 400 nm. During the friction process, a very thick lubricating film effectively prevents direct contact between the rough peaks, reducing the contact area and thereby enhancing the lubricating performance and lowering the coefficient of friction (Figure 9c). As the friction reaction proceeds, part of the friction film is transformed into fine particles with a height of about 300 nm through a friction chemical reaction process. These fine particles further reduce the contact area and enhance the load-bearing capacity, through their combined effects, a significant enhancement in lubricating performance was achieved.

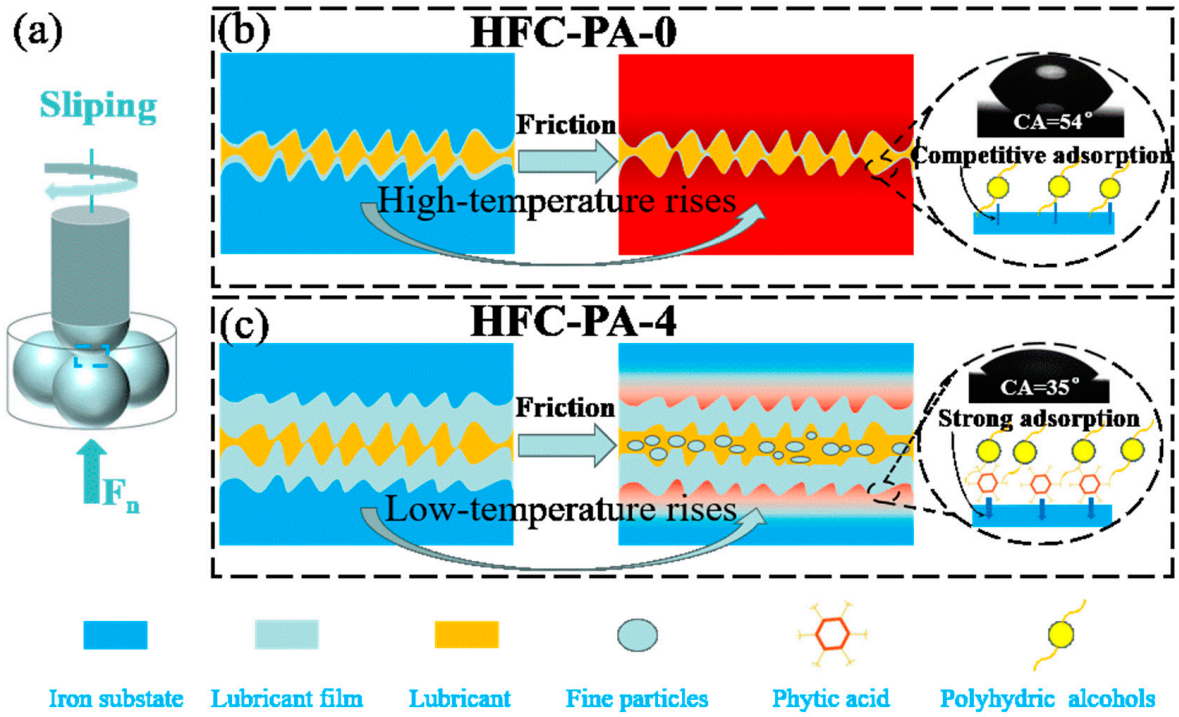


Figure 9. (**a**) Schematic diagram of the four-ball friction test, (**b**)The possible superlubrication mechanism of HFC-PA-0, (**c**) The possible superlubrication mechanism of HFC-PA-4.

4. Discussion

The HFC-PA-4 hydraulic fluid developed in this study, which contains phytic acid, achieved an ultra-low friction coefficient of 0.013 through a four-ball friction test, outperforming water-based hydraulic fluids reported in the literature (Figure 1c). This significant improvement is attributed to the strong adsorption of phosphate groups in phytic acid molecules onto the surface of GCr15 steel balls (Figure 9), forming a lubricating film with a thickness of 392 nm (Figure 5a), which is much higher than that of the control group without phytic acid (7 nm). XPS and TOF-SIMS analyses indicate that phytic acid undergoes tribochemical reactions with the steel surface during the friction process, generating phosphorus-containing compounds (such as $FePO_4$) and carbon-rich lubricating films (Figures 6 and 7). These films effectively isolate the direct contact between the friction pairs, thereby reducing friction and wear. Additionally, the lubricating film is transformed into micrometer-sized particles under shear action (Figure 8), which further enhances the load-bearing capacity through a rolling effect, synergistically reducing the friction coefficient.

The significant suppression of frictional heat (a 78.6% reduction in temperature rise) is directly related to the ultra-low friction coefficient (Figure 2). The reduction in frictional

force decreases energy dissipation, while the uniformity and thermal stability of the lubricating film further inhibit the formation of local hot spots. Compared with the commercial hydraulic fluid Castrol, the temperature rise advantage of HFC-PA-4 (9.0 °C vs. 35.4 °C) indicates its potential for application in high-temperature conditions. The biotoxicity test shows that the 96 h LC50 value of HFC-PA-4 (26,304 mg/L) is higher than that of Castrol (23,795 mg/L), confirming its low ecological risk. The natural origin and biodegradability of phytic acid further enhance the environmental friendliness of this hydraulic fluid, meeting the strict requirements for low biotoxicity in marine equipment.

Despite its excellent performance, the long-term stability of HFC-PA-4, such as the recyclability of microparticles, and its tribological behavior under extreme pressure still needs further verification. In the future, the durability of the lubricating film can be further improved through molecular structure optimization (such as the design of phytic acid derivatives), and its practical application potential in complex marine environments (such as high salinity and high pressure) can be explored.

5. Conclusions

Hydraulic technology has facilitated its widespread application in offshore mechanical equipment, particularly in drilling platforms and ships, where high-performance hydraulic fluids are crucial for safe and efficient operation. However, the development of water-based hydraulic fluids as an alternative to traditional oil-based hydraulic fluids, while achieving low biotoxicity, low coefficient of friction, and reduced frictional heat generation, has been an urgent issue that needs to be addressed. This study introduces the incorporation of phytic acid, a green organic compound derived from plant seeds, as a key component to reduce the coefficient of friction and frictional heat, compounded with commercial thickeners and additives to formulate a new type of water-based hydraulic fluid. The incorporation of phytic acid has significantly enhanced the lubricating performance, with the average coefficient of friction reduced to as low as 0.013 as tested by the four-ball tester, which is the lowest value reported to date. Concurrently, real-time monitoring of the temperature rise of the friction testing apparatus using an infrared thermal imager revealed a 78.6% reduction in temperature increase. Furthermore, Acute toxicity assays using Brine Shrimp demonstrated that the 96 h LC50 (half lethal concentration) value for the water–glycol flame-resistant hydraulic fluid with added phytic acid exceeded 26,304 mg/L, indicating low toxicity. Subsequent characterization analyses elucidated the mechanisms underlying the improved tribological properties.

Author Contributions: Conceptualization, Q.C.; Formal analysis, W.L., Q.C. and J.Y.; Funding acquisition, H.C., L.C., N.J. and T.C.; Investigation, W.L. and S.G.; Methodology, W.L., H.C. and T.C.; Resources, N.J. and T.C.; Software, W.L. and L.C.; Validation, S.G., G.G., J.Y., K.N. and T.C.; Visualization, W.L.; Writing—original draft, W.L.; Writing—review & editing, T.C. All authors have read and agreed to the published version of the manuscript.

Funding: This research was funded by the National Natural Science Foundation of China (52075527, 51573201, and U1709205) and the National Key R&D Program of China (2024YFB3816600 and 2024YFB3816604).

Institutional Review Board Statement: Not applicable.

Informed Consent Statement: Not applicable.

Data Availability Statement: The data that support the findings of this study are available from the corresponding author upon reasonable request.

Acknowledgments: We take this opportunity to express our gratitude for the support from the two platforms of Ningbo University and the Ningbo Institute of Materials Technology and Engineering of the Chinese Academy of Sciences.

Conflicts of Interest: The authors declare no conflicts of interest.

References

1. Du, Z.; Chen, X.; Zhang, Q.; Yang, Y. An extended state observer-based sliding mode control method for hydraulic servo system of marine stabilized platforms. *Ocean Eng.* **2023**, *279*, 114386.
2. Ni, S.; Tang, Y.; Wang, G.; Yang, L.; Lei, B.; Zhang, Z. Risk identification and quantitative assessment method of offshore platform equipment. *Energy Rep.* **2022**, *8*, 7219–7229.
3. Bailey, D.M.; Hopkins, C.R. Sustainable use of ocean resources. *Mar. Policy* **2023**, *154*, 105672. [CrossRef]
4. Zhang, T.; Yan, L.; Han, G.; Guizani, N.; Liu, J. Low-cost, long-endurance cooperative navigation based on "light" marine equipment in deep sea. *IEEE Netw.* **2020**, *35*, 222–228.
5. Deuster, S.; Schmitz, K. Bio-based hydraulic fluids and the influence of hydraulic oil viscosity on the efficiency of mobile machinery. *Sustainability* **2021**, *13*, 7570. [CrossRef]
6. Khoshvaght-Aliabadi, M.; Khoshvaght, M.; Rahnama, P. Thermal-hydraulic characteristics of plate-fin heat exchangers with corrugated/vortex-generator plate-fin (CVGPF). *Appl. Therm. Eng.* **2016**, *98*, 690–701.
7. Wen, X.; Peng, G.; Bai, P.; Yuan, N.; Yue, L.; Meng, Y.; Tian, Y.; Li, L.; Ding, J. Tribocorrosion behavior of GCr15 steel in water–glycol fire-resistant hydraulic fluids (HFC) containing seawater. *J. Mater. Res. Technol.* **2024**, *30*, 4682–4691.
8. Zheng, D.; Liu, Z. Tribological Properties of Different Carboxylates in Water-Glycol Hydraulic Fluid. *Tribol. Trans.* **2022**, *65*, 653–661.
9. Gong, P.; Wen, X.; Bai, P.; Yue, L.; Ding, J.; Tian, Y.; Li, L. Influence of Low Concentration Seawater on the Friction Corrosion Performance of Water–Glycol Fire-Resistant Hydraulic Fluid. *J. Bio-Tribo-Corros.* **2024**, *10*, 49. [CrossRef]
10. Zheng, Z.; Liu, X.; Huang, G.; Chen, H.; Yu, H.; Feng, D.; Qiao, D. Macroscale superlubricity achieved via hydroxylated hexagonal boron nitride nanosheets with ionic liquid at steel/steel interface. *Friction* **2022**, *10*, 1365–1381. [CrossRef]
11. Holmberg, K.; Erdemir, A. Influence of tribology on global energy consumption, costs and emissions. *Friction* **2017**, *5*, 263–284. [CrossRef]
12. Awang, N.; Ramasamy, D.; Kadirgama, K.; Najafi, G.; Sidik, N.A.C. Study on friction and wear of Cellulose Nanocrystal (CNC) nanoparticle as lubricating additive in engine oil. *Int. J. Heat Mass Transf.* **2019**, *131*, 1196–1204. [CrossRef]
13. Zheng, Z.; Guo, Z.; Liu, W.; Luo, J. Low friction of superslippery and superlubricity: A review. *Friction* **2023**, *11*, 1121–1137. [CrossRef]
14. Liang, H.; Liu, M.; Yin, T.; Zou, S.; Xia, X.; Hua, X.; Fu, Y.; Zhang, J.; Bu, Y.; Ren, X. Carbon Dots as Ligand Operons to Expand Cluster Size Distribution for High Load-bearing Liquid Superlubricity. *Adv. Funct. Mater.* **2024**, *34*, 2311600. [CrossRef]
15. Dou, X.; Koltonow, A.R.; He, X.; Jang, H.D.; Wang, Q.; Chung, Y.-W.; Huang, J. Self-dispersed crumpled graphene balls in oil for friction and wear reduction. *Proc. Natl. Acad. Sci. USA* **2016**, *113*, 1528–1533. [CrossRef]
16. Wong, V.W.; Tung, S.C. Overview of automotive engine friction and reduction trends–Effects of surface, material, and lubricant-additive technologies. *Friction* **2016**, *4*, 1–28. [CrossRef]
17. Laursen, J.L.; Sivebaek, I.M.; Christoffersen, L.W.; Papsoee, M.; Vigild, M.E.; Brondsted, P.; Horsewell, A. Influence of Tribological Additives on Friction and Impact Performance of Injection Moulded Polyacetal. *Wear* **2009**, *267*, 2294–2302. [CrossRef]
18. Camenzind, H.; Clark, D.; Dratva, A.; Fletschinger, M.; Ribeaud, M.; Rohrbach, P.; Reyes-Gavilan, J. New ashless, hydrolytically stable and FZG active antiwear agent. *Tribol. Trans.* **2002**, *45*, 223–231. [CrossRef]
19. Ellis, E.G. LUBRICANTS: An Industrial Health Hazard? *Ind. Lubr. Tribol.* **1967**, *19*, 141–145. [CrossRef]
20. San Kong, P.; Aroua, M.K.; Daud, W.M.A.W.; Cognet, P.; Pérès, Y. Enhanced microwave catalytic-esterification of industrial grade glycerol over Brønsted-based methane sulfonic acid in production of biolubricant. *Process Saf. Environ. Prot.* **2016**, *104*, 323–333. [CrossRef]
21. Peppou-Chapman, S.; Neto, C. Depletion of the lubricant from lubricant-infused surfaces due to an air/water interface. *Langmuir* **2021**, *37*, 3025–3037. [CrossRef] [PubMed]
22. Shao, L.; Li, Y.; Pan, F.; Zhang, Z.; Liang, S.; Wang, Y.; Zou, J.; Jiang, Z. Graphene oxide membranes tuned by metal-phytic acid coordination complex for butanol dehydration. *J. Membr. Sci.* **2021**, *638*, 119736. [CrossRef]
23. Wan, Y.; Yu, Y.; Gao, S.; Gao, J. Low friction of phytic acid as a water-based lubricant additive. *Ind. Lubr. Tribol.* **2017**, *69*, 1085–1090. [CrossRef]
24. Li, C.-c.; Guo, X.-y.; Shen, S.; Song, P.; Xu, T.; Wen, Y.; Yang, H.-F. Adsorption and corrosion inhibition of phytic acid calcium on the copper surface in 3 wt% NaCl solution. *Corros. Sci.* **2014**, *83*, 147–154. [CrossRef]

25. Lieberman, M. A Brine Shrimp Bioassay for Measuring Toxicity and Remediation of Chemicals. *J. Chem. Educ.* **1999**, *76*, 1689. [CrossRef]
26. Suman, T.Y.; Jia, P.-P.; Li, W.-G.; Junaid, M.; Xin, G.-Y.; Wang, Y.; Pei, D.-S. Acute and Chronic Effects of Polystyrene Microplastics on Brine Shrimp: First Evidence Highlighting the Molecular Mechanism through Transcriptome Analysis. *J. Hazard. Mater.* **2020**, *400*, 123220. [CrossRef]
27. Tang, G.; Wu, Z.; Su, F.; Wang, H.; Xu, X.; Li, Q.; Ma, G.; Chu, P.K. Macroscale superlubricity on engineering steel in the presence of black phosphorus. *Nano Lett.* **2021**, *21*, 5308–5315. [CrossRef] [PubMed]
28. You, X.; Wu, H.; Zhang, R.; Su, Y.; Cao, L.; Yu, Q.; Yuan, J.; Xiao, K.; He, M.; Jiang, Z. Metal-coordinated sub-10 nm membranes for water purification. *Nat. Commun.* **2019**, *10*, 4160. [CrossRef] [PubMed]
29. Dašić, M.; Almog, R.; Agmon, L.; Yehezkel, S.; Halfin, T.; Jopp, J.; Ya'akobovitz, A.; Berkovich, R.; Stanković, I. Role of Trapped Molecules at Sliding Contacts in Lattice-Resolved Friction. *ACS Appl. Mater. Interfaces* **2024**, *16*, 44249–44260. [CrossRef] [PubMed]
30. Gkagkas, K.; Ponnuchamy, V.; Dašić, M.; Stanković, I. Molecular Dynamics Investigation of a Model Ionic Liquid Lubricant for Automotive Applications. *Tribol. Int.* **2017**, *113*, 83–91. [CrossRef]
31. Yang, Z.; Guo, J.; Dang, P.; Gong, B. Tribological properties of GO/modified SiO2 combination as lubricant additive for bearings. *Tribol. Int.* **2024**, *199*, 109946. [CrossRef]
32. Wang, J.; Li, X.; Deng, Y.; Chen, S.; Liang, W.; Zhang, L.; Wei, X.; Gao, S.; Wan, Y. Carbon quantum dots doped with silver as lubricating oil additive for enhancing tribological performance at various temperatures. *Appl. Surf. Sci.* **2022**, *599*, 154029. [CrossRef]
33. Advincula, P.A.; Granja, V.; Wyss, K.M.; Algozeeb, W.A.; Chen, W.; Beckham, J.L.; Luong, D.X.; Higgs III, C.F.; Tour, J.M. Waste plastic-and coke-derived flash graphene as lubricant additives. *Carbon* **2023**, *203*, 876–885. [CrossRef]
34. Meng, Y.; Sun, J.; He, J.; Yang, F.; Wu, P. Interfacial interaction induced synergistic lubricating performance of MoS2 and SiO2 composite nanofluid. *Colloids Surf. A Physicochem. Eng. Asp.* **2021**, *626*, 126999. [CrossRef]
35. Guo, Y.-F.; Zhang, H.-T.; Liu, Y.-W.; Zhou, X.-F.; Liu, Z.-P. Molecular-scale grinding of uniform small-size graphene flakes for use as lubricating oil additives. *New Carbon Mater.* **2023**, *38*, 954–963. [CrossRef]
36. Wu, P.-R.; Liu, Z.; Cheng, Z.-L. Growth of MoS2 Nanotubes Templated by Halloysite Nanotubes for the Reduction of Friction in Oil. *ACS Omega* **2018**, *3*, 15002–15008. [CrossRef] [PubMed]
37. Zu, P.; Zhang, Y.; Zhang, S.; Li, Y.; Hu, L. Excellent corrosion inhibition and lubrication performance of MMT based ionic liquids as ester oil additives. *Tribol. Int.* **2024**, *194*, 109473. [CrossRef]
38. Song, W.; Yan, J.; Ji, H. Fabrication of GNS/MoS2 composite with different morphology and its tribological performance as a lubricant additive. *Appl. Surf. Sci.* **2019**, *469*, 226–235. [CrossRef]
39. Ravikiran, N.; Padya, B.; Junaid, S.; Jain, P.K.; Srikanth, V.V. Sustainable Kilogram-Scale Conversion of Tire Pyrolysis Waste into Nanosized Onion-like Carbons with Extraordinary Lubricant-Additive Properties. *ACS Sustain. Chem. Eng.* **2023**, *11*, 12045–12051. [CrossRef]
40. Zeng, L.; Li, X.; Shi, Y.; Qi, Y.; Huang, D.; Tadé, M.; Wang, S.; Liu, S. FePO4 based single chamber air-cathode microbial fuel cell for online monitoring levofloxacin. *Biosens. Bioelectron.* **2017**, *91*, 367–373. [CrossRef]
41. Castro, L.; Dedryvère, R.; El Khalifi, M.; Lippens, P.E.; Bréger, J.; Tessier, C.; Gonbeau, D. The spin-polarized electronic structure of LiFePO4 and FePO 4 evidenced by in-lab XPS. *J. Phys. Chem. C* **2010**, *114*, 17995–18000. [CrossRef]
42. Wang, Y.; Sherwood, P. Iron (III) phosphate (FePO4) by XPS. *Surf. Sci. Spectra* **2002**, *9*, 99–105. [CrossRef]
43. Xia, Y.; Zhang, S.; Wang, Z.; Zhang, C. New Insight into Tribofilm Composition and Structure of Iron Polyphosphate-Rich Tribofilm from Formulated Engine Oil by ToF-SIMS. *J Mater Sci* **2024**, *59*, 9533–9546. [CrossRef]
44. Britt, L.G.H.; Jenke, P.K.; Lipinsky, D.; Arlinghaus, H.F. ToF-SIMS Investigation of Tribochemical Surface Reaction Films Built up by Specially Added Cooling Lubricants. *J. Vac. Sci. Technol. B* **2018**, *36*, 03F120. [CrossRef]
45. Dašić, M.; Stanković, I.; Gkagkas, K. Molecular dynamics investigation of the influence of theshape of the cation on the structure and lubrication properties of ionic liquids. *Phys. Chem. Chem. Phys.* **2019**, *21*, 4375–4386. [CrossRef] [PubMed]
46. Dašić, M.; Stanković, I.; Gkagkas, K. Influence of Confinement on Flow and Lubrication Properties of a Salt Model Ionic Liquid Investigated with Molecular Dynamics. *Eur. Phys. J. E* **2018**, *41*, 130. [CrossRef]
47. Dašić, M.; Ponomarev, I.; Polcar, T.; Nicolini, P. Tribological Properties of Vanadium Oxides Investigated with Reactive Molecular Dynamics. *Tribol. Int.* **2022**, *175*, 107795. [CrossRef]

Disclaimer/Publisher's Note: The statements, opinions and data contained in all publications are solely those of the individual author(s) and contributor(s) and not of MDPI and/or the editor(s). MDPI and/or the editor(s) disclaim responsibility for any injury to people or property resulting from any ideas, methods, instructions or products referred to in the content.